School of Pharmacy, Shanghai University of Traditional Chinese Medicine, Shanghai, China

Preparation and *in vitro* anti-tumor properties of toad venom extract-loaded solid lipid nanoparticles

Su-Juan Zhang, Yong-Tai Zhang, Ji-Hui Zhao, Li-Na Shen, Feng Shi, Nian-Ping Feng

Received November 8, 2012, accepted January 13, 2013

Nian-Ping Feng, School of Pharmacy, Shanghai University of Traditional Chinese Medicine, Shanghai, China
npfeng@hotmail.com

Pharmazie 68: 653–660 (2013) *doi: 10.1691/ph.2013.2216*

In this study, we prepared solid lipid nanoparticles (TV-SLNs) loaded with toad venom extract and investigated their anti-tumor effects *in vitro* in HeLa and SKOV-3 cells. TV-SLNs were prepared using a cold homogenization technique, and the formulation was optimized by central composite design and response surface methods. The anti-tumor activities of TV-SLNs were evaluated by analyzing cell division and cell cycle distribution by using the MTT assay and flow cytometry. After incubation with TV-SLNs, the growth of both HeLa and SKOV-3 cells was inhibited significantly. The percentage of HeLa cells in G_0/G_1 phase decreased, whereas that in the S and G_2/M phases increased. Thus, the S and G_2/M phases were blocked after the incubation of HeLa cells with TV-SLNs for 24 h. In contrast, the percentage of SKOV-3 cells in G_0/G_1 phase increased and then decreased in S and G_2/M phases, with the G_0/G_1 phase being blocked after incubation with TV-SLNs for 24 h. Our results demonstrate that TV-SLNs inhibited the fissiparism of HeLa and SKOV-3 cells in a time-and dose-dependent manner. TV-SLNs may be effective as a novel TV vaginal delivery system for the treatment of cervical and ovarian cancers.

1. Introduction

Cervical cancer is a common female malignant tumor, with more than 200 000 women dying of cervical cancer worldwide every year. In developing countries, cervical cancer ranks first among gynecological tumors, followed by ovarian cancer and uterine body carcinoma (Haas et al. 2012; Qureshi and Saavedra 2011). There is a pressing need for alternative treatments with fewer side effects for cervical cancer, and the use of natural products is an interesting option, given the recent interest shown by the general population in natural drugs.

Toad venom (TV) is the dried venom obtained from the skin secretions of the *Bufo bufo gargarizans* Cantor or the *Bufo melanostictus* Schneider (Chinese Pharmacopoeia 2010; Ma et al. 2009), and is widely used in Chinese medicine to treat various cancers. Cinobufagin (CBG) and resibufogenin (RBG) are the 2 main active ingredients in TV with significant anti-tumor effects (Cao et al. 2007; Shimizu et al. 2004), including the inhibition of proliferation and angiogenesis in tumor endothelial cells (Plummer et al. 2012; Skarda et al. 2012; Yamada et al. 1998), and reversal of multidrug resistance (Peng et al. 2012). TV, as well as CBG and RBG, have been used to treat cervical and ovarian cancers (Masuda et al. 1995). However, when administered on the mucosa, severe irritation and toxicity have been reported to be induced by TV (Brubacher et al. 1996, 1999; Chan et al. 1995; Ma et al. 2012), thus limiting the clinical application of TV as an effective anticancer agent with conventional formulations.

Solid lipid nanoparticles (SLNs) have received a great deal of attention as a novel sustained-release delivery system for many therapeutic agents (Qi et al. 2012). SLNs consist of a biocompatible lipid core and a surfactant as the outer shell, which can increase drug solubility and bioavailability and improve physical stability and biocompatibility (Baviskar et al. 2012; Zhang et al. 2011). SLNs have been proposed as an alternative colloidal drug delivery system, particularly for drugs that possess narrow therapeutic windows. With a solid oil core matrix, drug molecules can be released from SLNs in a sustained manner, and may ultimately increase therapeutic safety and reduce side effects (Baviskar et al. 2012; Shegokar and Singh 2011).

In this study, SLNs were used as a vehicle for the TV extract to investigate their potential use in the vaginal delivery of TV for the treatment of cervical and ovarian cancers. Central composite design (CCD) was used to optimize the formulation. The *in vitro* anti-tumor activity of SLNs loaded with TV extract was compared with that of an aqueous suspension of TV extract by using the MTT assay and conducting cell cycle experiments in HeLa and SKOV-3 cells.

2. Investigation, results and discussion

2.1. Preparation and characterization of TV-SLNs

CCD factorial design is considered an effective experimental design strategy that is associated with a minimum number of experiments to estimate the influence of individual variables, and has been successfully implemented in the systematic optimization of various drug delivery systems (Dhawan et al. 2011). The concentrations of Compritol® 888 ATO (X_1), soyabean lecithin (Lipoid S 100) (X_2), and Pluronic® F68 (X_3) were chosen as factors in this experimental design. According to our preliminary experimental results, the principle of CCD and the feasibility of preparing the TV-SLNs under the highest or the lowest factor levels, with 5 levels of each factor, were determined as shown in Table 1. Entrapment efficiency (EE), drug loading, and mean

Table 1: Variables and observed responses in the central composite design for solid lipid nanoparticles (SLNs)

Formulation	Independent variables			Dependent variables			
	X_1	X_2	X_3	Y_1 (%)	Y_2 (%)	Y_3 (nm)	Y_4
SLN1	−1	−1	−1	93.41	1.64	79.35	0.40
SLN2	1	−1	−1	68.74	0.74	90.12	0.31
SLN3	−1	1	−1	55.05	0.71	44.29	0.33
SLN4	1	1	−1	83.72	0.57	36.13	0.35
SLN5	−1	−1	1	88.79	1.37	146.00	0.35
SLN6	1	−1	1	91.24	0.82	259.60	0.31
SLN7	−1	1	1	84.22	0.87	73.26	0.35
SLN8	1	1	1	96.75	0.66	245.50	0.34
SLN9	−1.732	0	0	77.29	1.26	114.30	0.32
SLN10	1.732	0	0	98.16	0.76	222.90	0.36
SLN11	0	−1.732	0	82.97	1.06	401.30	0.22
SLN12	0	1.732	0	87.19	0.66	32.02	0.37
SLN13	0	0	−1.732	82.03	0.93	32.57	0.35
SLN14	0	0	1.732	93.94	0.79	71.21	0.39
SLN15	0	0	0	84.33	0.84	70.52	0.35
SLN16	0	0	0	89.92	0.96	133.90	0.36
SLN17	0	0	0	81.66	0.91	295.40	0.19
SLN18	0	0	0	84.01	1.08	71.36	0.35
SLN19	0	0	0	83.90	1.20	51.28	0.36
SLN20	0	0	0	86.69	1.19	56.48	0.37
Independent variables	Levels used, actual (coded)						
	−1.732	−1	0	1	+1.732		
X_1 = Compritol® 888 ATO (%, w/v)	0.50	1.13	2.00	2.87	3.50		
X_2 = Lipoid S 100 (%, w/v)	0.50	0.92	1.50	2.08	2.50		
X_3 = Pluronic® F68 (%, w/v)	0.50	0.92	1.50	2.08	2.50		

Y_1, encapsulation efficiency of toad venom extract-loaded SLN (TV-SLN); Y_2, drug loading of TV-SLN; Y_3, mean particle size of TV-SLN.

particle size of the TV-SLNs were selected as experimental indicators and designated as Y_1, Y_2, and Y_3, respectively. A comprehensive experimental index (Y_4) of overall desirability was introduced to investigate the comprehensive effects of Y_1 to Y_3, and the data were normalized according to the Hassan equation (Goretti et al. 2012). The experimental values of the responses are shown in Table 1. The four response variables measured in this study demonstrated a good fit with the multiple linear regression models ($p < 0.05$). The equations used were as follows: $Y_1 = 54.370 + 5.107 \times X_1 - 1.753 \times X_2 + 15.159 \times X_3$ ($r = 0.626$, $p = 0.042$); $Y_2 = 1.873 - 0.232 \times X_1 - 0.0318 \times X_2 + 0.014 \times X_3$ ($r = 0.796$, $p = 0.001$); $Y_3 = 38.972 + 42.660 \times X_1 - 114.990 \times X_2 + 116.790 \times X_3$ ($r = 0.6685$, $p = 0.015$); and $Y_4 = 0.906 - 0.009 \times X_1 + 0.117 \times X_2 - 0.035 \times X_3$ ($r = 0.759$, $p = 0.002$).

With regard to the Y_1 to Y_3 equations, X_1 had the largest effect on the responses of Y_1, Y_2, and Y_3, demonstrating that the concentration of Compritol® 888 ATO affects the EE and size distribution of TV-SLN markedly, whereas the negative correlation to drug loading was comparatively lower. Reports have demonstrated that using Compritol® 888 ATO as the lipid core of SLNs is conducive to the formation of a stable dispersion with a smaller particle size (Dhawan et al. 2011; Kakkar et al. 2011; Kaur et al. 2008). X_2 showed the largest antagonistic effect on the responses of Y_3, with the concentration of Lipoid S 100 being less important to the mean particle size of TV-SLN, and a larger negative correlation to the EE of TV-SLN. X_3 demonstrated the largest synergistic effect on the responses of Y_1 and Y_3, showing that the concentrations of Pluronic® F68 can influence the EE and mean particle size of TV-SLN greatly. Similar findings of smaller mean particle size with increased surfactant concentration were described by Weyenberg and Castro and colleagues (Castro et al. 2009; Weyenberg et al. 2007). The augmented loading of TV through an increase in surfactant concentration suggested that TV might be embedded in the surfactant layer, rather than be incorporated into the lipid matrix (Castro et al. 2009). A positive correlation between X_2 and Y_4 was found from the equation for Y_4, indicating that among the three experimental factors, only the concentration of Lipoid S 100 affected all of the indicators.

Based on the multiple linear regression equations, the three-dimensional response surface curves and the two-dimensional contour curves for Y_1, Y_2, Y_3, and Y_4 were determined (Fig. 1). Optimization was performed by superimposing the contour plots of the Y_1, Y_2, and Y_3 responses, and locating the region of optimal surface that was common to all of the plots.

The five formulations that were prepared based on the optimum region identified are shown in Table 2. The mean particle sizes ranged from 120.2 ± 4.98 nm to 145.6 ± 3.74 nm, and the mean particle size of the drug-loaded TV-SLNs was larger than that of SNLs without the drug. A similar phenomenon was reported by Lu et al. (2006), and may be attributed to the embedding of the drug in the interfacial film (Chen et al. 2004; Jiang et al. 2012). The nanoparticles displayed a spherical shape and remained separate from each other (Fig. 2).

The experimental values approximated the predicted values, showing that the optimal surface was chosen correctly and that the model was suitable for optimization of the formulations. Formulation 1, which contained 2.0% (w/v) Compritol® 888 ATO, 2.0% (w/v) Lipoid S 100, and 2.0% (w/v) Pluronic® F68, obtained the highest values for EE ($92.97 \pm 0.57\%$) and drug loading ($0.79 \pm 0.08\%$), with a size distribution of 127.8 ± 2.14 nm,

Table 2: Composition of the toad venom extract-loaded solid lipid nanoparticles (TV-SLNs) checkpoint formulations, and the predicted and experimental values of the response variables and bias values (n = 3)

Formulation	Predicted values			Experimental values			Bias		
	Y_1 (%)	Y_2 (%)	Y_3 (nm)	Y_1 (%)	Y_2 (%)	Y_3 (nm)	Y_1 (%)	Y_2 (%)	Y_3 (%)
1	92.35	0.76	133.70	92.97 ± 0.57	0.79 ± 0.08	127.80 ± 2.14	0.67	3.60	4.35
2	90.71	0.80	127.20	91.57 ± 0.62	0.64 ± 0.13	145.60 ± 3.74	0.95	20.00	14.47
3	88.22	0.62	115.60	88.14 ± 1.27	0.65 ± 0.02	120.20 ± 4.98	0.09	4.84	3.98
4	89.10	0.67	145.10	90.10 ± 0.95	0.65 ± 0.01	141.00 ± 5.97	1.12	2.99	2.93
5	91.54	0.71	134.50	92.07 ± 0.47	0.69 ± 0.19	131.80 ± 2.79	0.58	2.82	2.01
Composition				Formulation					
				1	2	3	4	5	
Compritol® 888 ATO (%, w/v)				2.00	1.50	0.50	1.00	2.50	
Lipoid S 100 (%, w/v)				2.00	1.80	0.50	1.20	2.50	
Pluronic® F68 (%, w/v)				2.00	2.00	0.50	1.00	2.50	

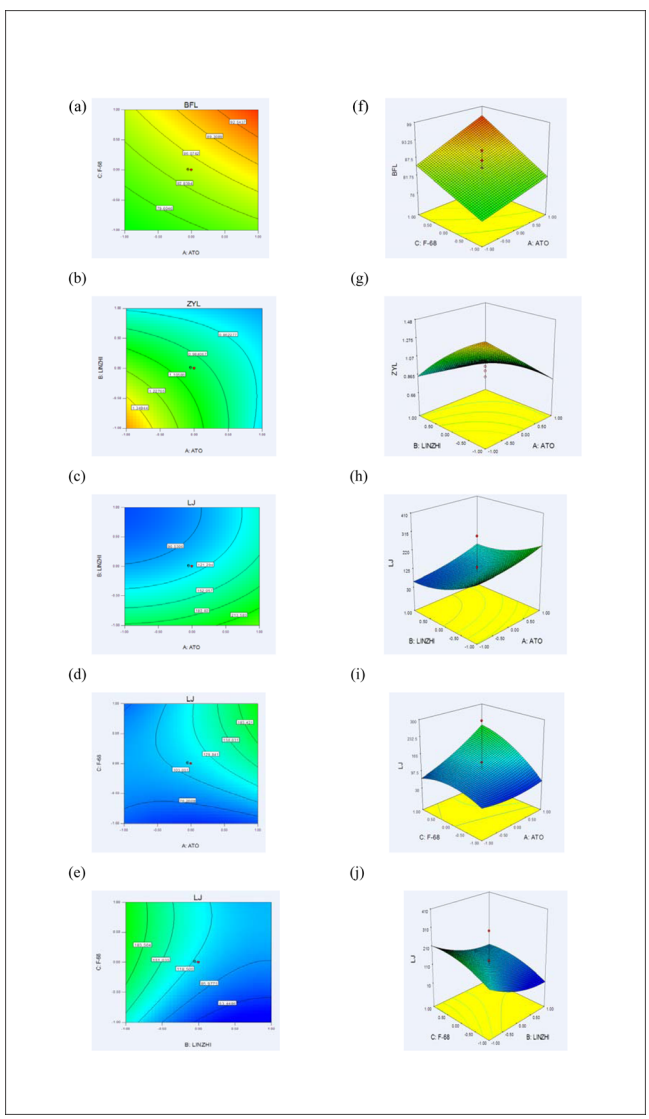

Fig. 1: Contour plot showing the effects of (a) X_1 (Compritol® 888 ATO [ATO]) and X_3 (Pluronic® F68 [F-68]) on response Y_1 (entrapment efficiency [EE]); (b) X_1 and X_2 (Lipoid S 100 [LINZHI]) on response Y_2 (drug loading); and (c) X_1 and X_2, (d) X_1 and X_3, (e) X_2 and X_3 on response Y_3 (mean particle size). The corresponding response surface plots are shown in (f)-(j)

and was therefore selected as the optimized formulation for further studies.

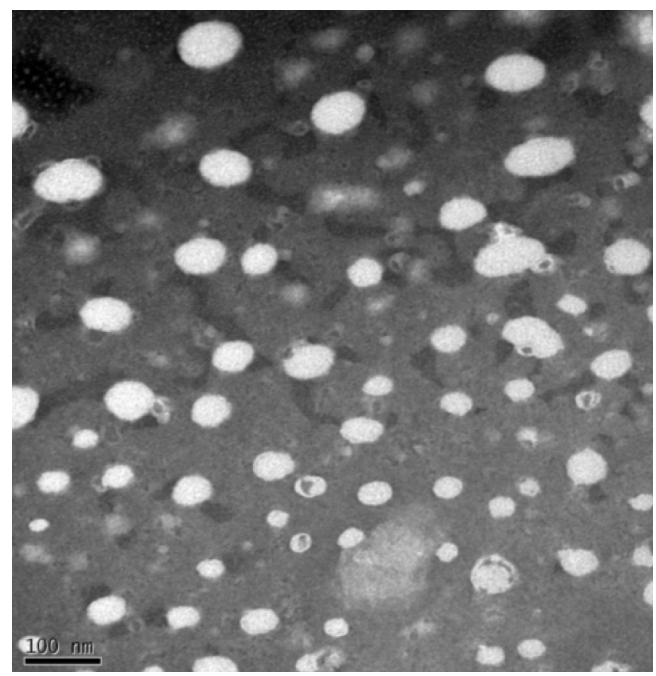

Fig. 2: Transmission electron microscopy of toad venom extract-loaded solid lipid nanoparticles (TV-SLNs)

2.2. *In vitro anti-tumor studies*

As shown in Fig. 3, elongated and polygonal-shaped HeLa cells were observed regularly, whereas the SKOV-3 cells were round in appearance. However, the inhibition of cell growth by the TV-SLN and TV extract suspensions resulted in gradual changes to the cytomorphology of the cells, with elliptical or horseshoe-shaped cells being observed. Moreover, after incubation with TV-SLNs, cell clarity appeared to decrease, ecthyma on the edge of cell membranes was observed in HeLa cells, and several SKOV-3 cells appeared to change into empty bubbles. These observations became more prevalent with increasing concentrations of TV-SLNs.

The inhibition effects of the TV incorporated in SLNs on HeLa and SKOV-3 cells were further examined using the MTT assay. As shown in Fig. 4, and Tables 3 and 4, both the TV-SLN and TV extract suspensions significantly ($p < 0.05$) inhibited the proliferation of HeLa and SKOV-3 cells in a dose- and time-dependent manner. After incubation for 24 h, the median inhibitory concentration (IC_{50}) of the TV extract suspension was 527.06 ng/mL in HeLa cells and 2040.71 ng/mL in SKOV-3 cells. These IC_{50} values were approximately 10-fold and 13-fold higher than that of

Table 3: The optical densities (at 490 nm) of HeLa and SKOV-3 cells treated with MTT after exposure to toad venom extract-loaded solid lipid nanoparticles (TV-SLNs) for different incubation times (n = 5)

Cells	Concentration (ng/mL)	Incubation time (h)		
		24	48	72
HeLa	Control	0.338 ± 0.041	0.738 ± 0.045	1.265 ± 0.142
	5.88	$0.249 \pm 0.033^*$	$0.390 \pm 0.037^*$	$0.714 \pm 0.173^*$
	58.79	$0.146 \pm 0.023^*$	$0.238 \pm 0.040^*$	$0.265 \pm 0.043^*$
	587.89	$0.091 \pm 0.015^*$	$0.201 \pm 0.043^*$	$0.234 \pm 0.057^*$
	5878.89	$0.062 \pm 0.012^*$	$0.177 \pm 0.034^*$	$0.206 \pm 0.026^*$
	58788.95	$0.073 \pm 0.010^*$	$0.105 \pm 0.023^*$	$0.114 \pm 0.003^*$
SKOV-3	Control	0.071 ± 0.021	0.214 ± 0.015	0.254 ± 0.022
	5.88	$0.055 \pm 0.003^*$	$0.207 \pm 0.025^*$	$0.133 \pm 0.018^*$
	58.79	$0.034 \pm 0.004^*$	$0.143 \pm 0.020^*$	$0.034 \pm 0.018^*$
	587.89	$0.031 \pm 0.004^*$	$0.082 \pm 0.011^*$	$0.047 \pm 0.009^*$
	5878.89	$0.023 \pm 0.001^*$	$0.070 \pm 0.002^*$	$0.027 \pm 0.011^*$
	58788.95	$0.011 \pm 0.001^*$	$0.022 \pm 0.012^*$	$0.024 \pm 0.012^*$

* $p < 0.05$, compared with the control group.

TV-SLNs in HeLa and SKOV-3 cells, respectively. Therefore, SLNs appeared to enhance the anti-tumor effect of TV (Sintov and Shapiro 2004). Similar results were reported in studies by Zhuang et al. (2012) with SLNs of anticancer drugs against the MCF-7 cell line. Studies have demonstrated that SLNs may affect the biodistribution of the incorporated drugs and thereby affect their *in vivo* performance; this may be due to the lipidic composition of the particular surface characteristics of SLNs, leading to their effective interaction with biomembranes and their biodistribution (Qi et al. 2012). For the SLNs prepared in the study by Qi et al. (2012), an average particle size of less than 200 nm and a spherical shape were shown to enhance the absorption of the cancer cells *in vitro*. The Lipoid S 100 surfactant, which is composed of a high purity of phosphatidylcholine (> 95%, w/w), that was used in the SLNs was similar to the cytomembrane, possibly increasing the biocompatibility between the SLNs and the cells, and thus increasing the uptake of TV incorporated in SLNs. The greater uptake of TV in HeLa or SKOV-3 cells via SLNs compared with free drug formulations may contribute to higher cytotoxicity *in vitro*.

The results from the cell cycle detection experiments are presented in Fig. 5, and the histograms created by flow cytometry are displayed in Fig. 6. Compared with the control group, the percentage of HeLa cells in the G_0/G_1 phase decreased from 74.41 ± 0.54 % to 22.16 ± 0.26 % after incubation with TV-SLN or TV extract suspensions, and increased from 21.74 ± 0.30% to 32.87 ± 0.41% in the S phase and from 3.86 ± 0.32% to 44.37 ± 0.21% in the G_2/M phase. These changes in the cell cycle population were dose-dependent (Fig. 5a and 6). TV has been shown to inhibit the DNA synthesis of HeLa cells in S phase, interfere with karyokinesis, and thus, restrain the proliferation of tumor cells (Minelli et al. 2012).

Table 4: The median inhibitory concentration (IC_{50}) values of HeLa and SKOV-3 cells treated with toad venom extract-loaded solid lipid nanoparticles (TV-SLNs) for different incubation times (n = 5)

Cells	Treatment	IC_{50} (ng/mL)		
24 h	48 h	72 h		
HeLa	TV-SLN	55.26	9.29	3.82
TV extract	526.75	109.94	41.62	
SKOV-3	TV-SLN	179.31	40.51	2.41
TV extract	2404.47	532.04	34.27	

The percentage of SKOV-3 cells in the G_0/G_1 phase increased from 46.46 ± 0.26% to 76.81 ± 0.30 % after incubation with TV-SLN and TV extract suspensions, and decreased from 41.21 ± 0.33% to 20.95 ± 0.36% in S phase and from 12.33 ± 0.24% to 2.36 ± 0.36% in the G_2/M phase (Fig. 5b and 6). Compared with the control cells, SKOV-3 cells showed dramatic cell cycle arrest in the G_0/G_1 phase ($p < 0.05$). TV may induce SKOV-3 cells to enter into the G_0/G_1 phase, and delay their passage into S phase. Similar to HeLa cells, SKOV-3 cells showed a dose-dependent cell cycle effect of TV. As shown by the MTT assay results presented in Fig. 4, compared with TV extract, TV-SLNs exhibited enhanced inhibitory activity in both HeLa and SKOV-3 cells ($p < 0.05$).

SLNs have been reported to have better biocompatibility with normal cells, such as Caco-2 cells (Silva et al. 2011). Nanoparticles with a mean particle size of less than 200 nm can bypass first-pass metabolism by the liver, which is generally considered the major site of drug degradation (Kakkar et al. 2011). Moreover, a smaller particle size can favor the absorption of transdermal, ocular, or pulmonary delivery (Qi et al. 2012). In addition, the surfactants used with soybean lecithin (Lipoid S 100) and Pluronic® F68 in the prepared SLNs may provide an improvement in the permeability of the vaginal membrane or in the affinity between lipid particles and the vaginal membrane, and may also enhance bioadhesion to the vaginal wall. Loaded the drug in SLNs can also result in controlled release after being applied topically (Baviskar et al. 2012), and the formulated TV loaded SLNs may reduce the irritation from TV as well as modulate drug release for topical use, such as vaginal or transdermal delivery (Castro et al. 2009; Guo et al. 2011).

In conclusion, the CCD method was shown to be suitable for the optimization of TV-SLN formulations, and resulted in an optimized TV-SLN formulation with enhanced EE and drug-loading properties. TV-SLN was found to enhance the inhibitory activity of TV in both HeLa and SKOV-3 cells *in vitro*. Therefore, SLNs may be effective as a novel vaginal delivery system for TV in the treatment of cervical and ovarian cancers.

3. Experimental

3.1. Materials

TV was provided by Sanyitang Chinese Medicinal Slices Co. Ltd (Bozhou, China), and extracted with alcohol. The TV extract contained 17.01% (w/w) RBG and CBG. Standard references (purity ≥ 98%, determined by HPLC) for RBG and CBG were provided by Linuo Biotechnology Co. Ltd (Zhengzhou, China). Compritol® 888 ATO and Pluronic® F68 were pur-

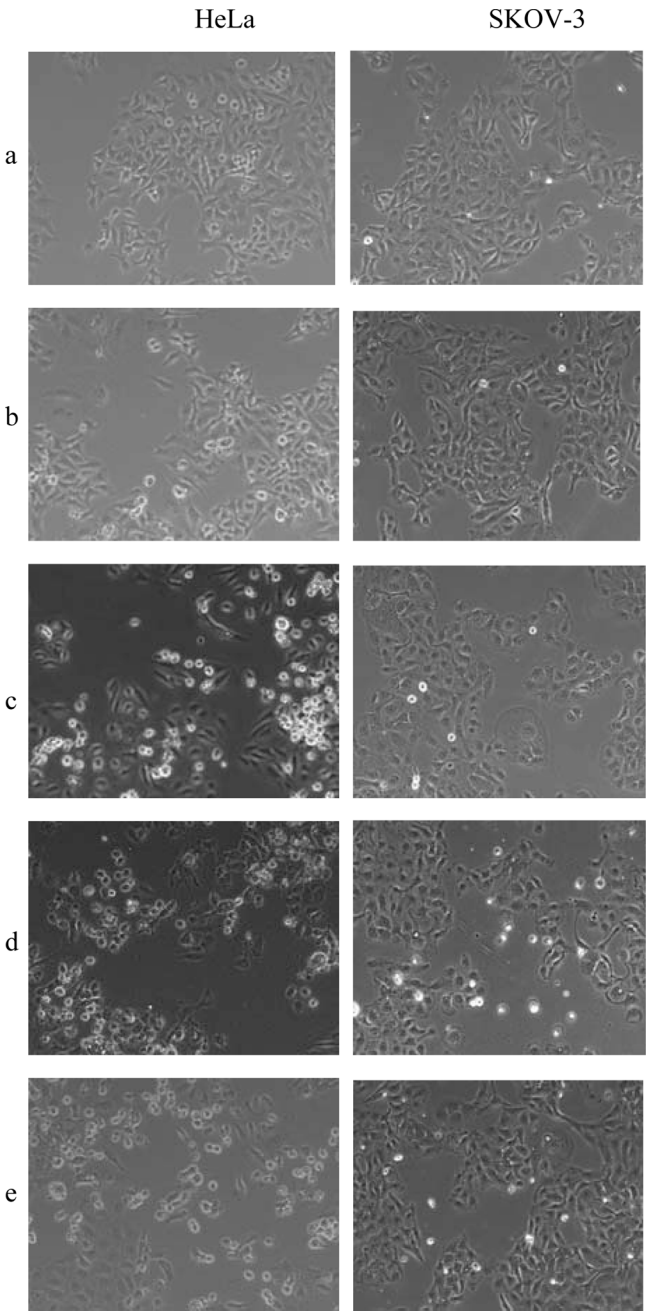

Fig. 3: Microphotographs of HeLa and SKOV-3 cells after incubation with toad venom extract-loaded solid lipid nanoparticles (TV-SLNs) for different time periods. (a) Control cells incubated without any drugs for 24 h; (b), (c), and (d), cells incubated for 24 h with 5.88 ng/mL, 58.82 ng/mL, or 588.24 ng/mL TV-SLN, respectively; and (e) cells incubated with 588.24 ng/mL TV extract for 24 h (× 200)

chased from BASF (Ludwigshafen, Germany). Lipoid S 100 containing 95.8% phosphatidylcholine (from soybean lecithin) was kindly provided by Lipoid GmbH (Ludwigshafen, Germany). High-glucose Dulbecco's Modified Eagle's Medium (DMEM/High, Fisher Scientific Worldwide [Shanghai] Co. Ltd, Shanghai, China), 0.25% trypsin, 0.02% EDTA, fetal calf serum, and phosphate buffer solution (PBS) were obtained from Shanghai Usen Biotechnology (Shanghai, China). L-Glutamine, antibiotics, and bovine serum albumin were purchased from Life Technologies Corporation (Orlando, FL, USA). A cell death detection kit (POD) was obtained from Chemicon International Inc. (Temecula, CA, USA). MTT (3-[4,5-dimethylthiazol-2-yl]-2,5-diphenyltetra-zolium bromide) was purchased from Shanghai Weihong Biological Technology Co. Ltd (Shanghai, China). All other chemicals were obtained from Sinopharm Chemical Reagent Co. Ltd (Shanghai, China) and were of HPLC or analytical grade.

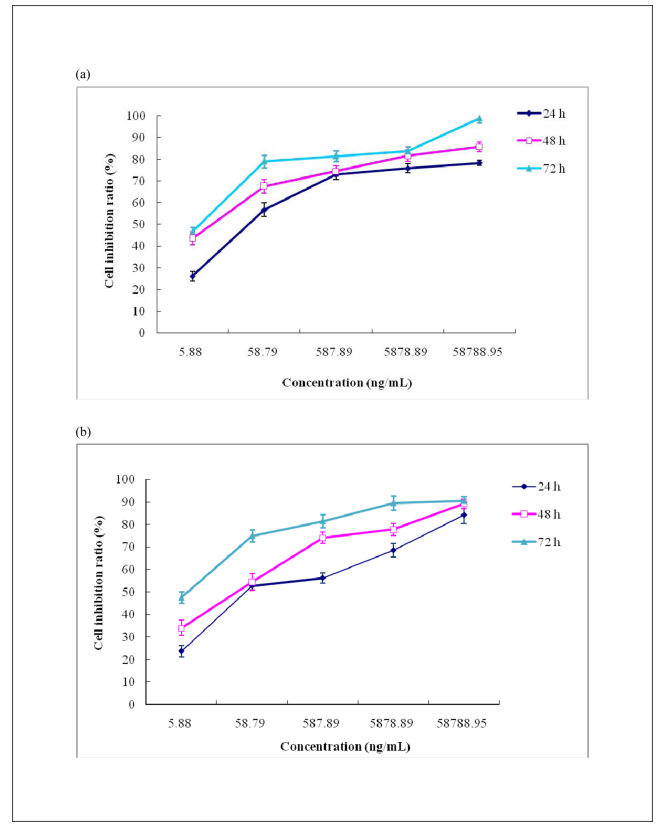

Fig. 4: The inhibition ratios of toad venom extract-loaded solid lipid nanoparticles (TV-SLNs) on cell growth in HeLa (a) and SKOV-3 (b) cells. Cell growth was determined using the MTT assay and the results are expressed as the percentage of cell growth relative to untreated control cells (n = 5)

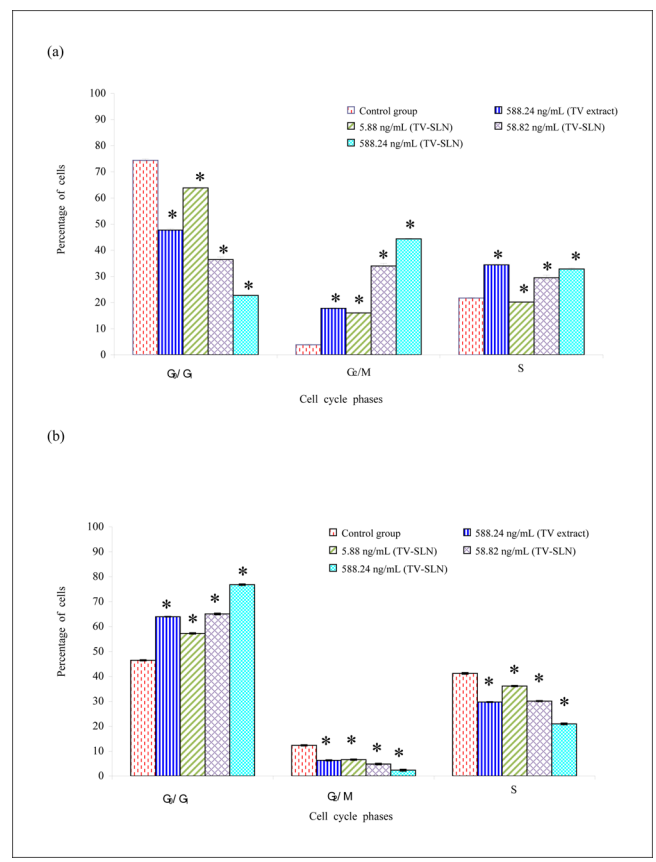

Fig. 5: Cell cycle distribution of HeLa (a) and SKOV-3 (b) cells incubated with toad venom extract-loaded solid lipid nanoparticles (TV-SLNs) for 24 h compared with the untreated control group (n = 5). *$p < 0.05$

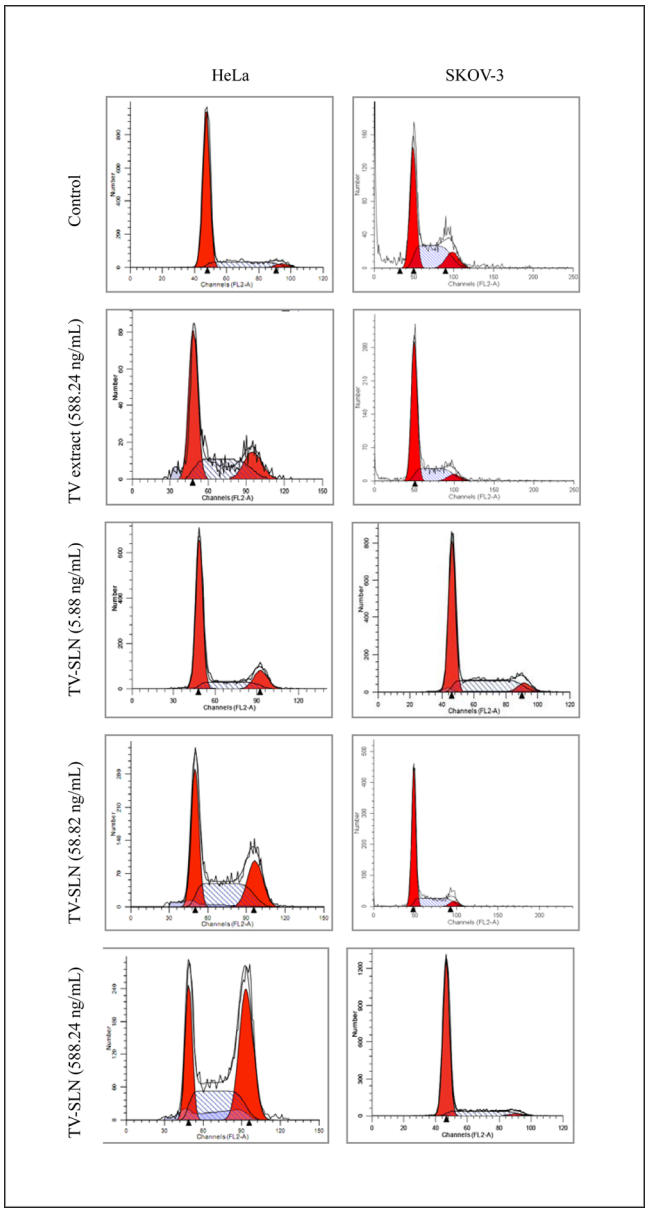

Fig. 6: The representative cell cycle profiles of HeLa (A) and SKOV-3 (B) cells incubated with toad venom extract-loaded solid lipid nanoparticles (TV-SLNs) and TV extract suspensions for 24 h. (G_0/G_1 dip, S dip, G_2/M dip)

3.2. Cell lines

HeLa cells, a human cervical cancer cell line, and SKOV-3 cells, a human ovarian cancer cell line, were purchased from the Shanghai Institute of Biochemistry and Cell Biology (Shanghai, China).

3.3. HPLC analysis of CBG and RBG

The LC-2010A HT Liquid Chromatograph system (Shimadzu Corporation, Kyoto, Japan) was used to detect the presence and determine the concentrations of CBG and RBG in the samples. An Ultimate® XB-C18 reverse phase column (5 μm, 4.6 mm inner diameter × 250 mm; Welch Materials, Inc., Shanghai, China) and an ultraviolet detector (Hamamatsu Photonics, Hamamatsu, Japan) were used in the HPLC analysis. The mobile phase consisted of methanol:water (55:45, v/v) with a flow of 1 mL/min. The column temperature was kept constant at 40 °C and the detection wavelength used was 296 nm. The recovery percentage ranged from 94.18 to 101.40 % for CBG and RBG. The intra-day relative standard deviation (SD) values were 0.11% and 0.14% for CBG and RBG, respectively, whereas the inter-day relative SD values were 1.22% and 0.82% for CBG and RBG, respectively. The samples from the *in vitro* experiments were filtered through a nylon, 0.45-μm pore, disposable syringe filter (diameter: 13 mm, Shanghai Anpel Scientific Instrument Inc., Shanghai, China) before being automatically injected into the HPLC system.

3.4. Preparation of TV-SLNs

The TV-SLN suspensions were prepared using the cold-homogeneity method. TV extract, Compritol® 888 ATO, and Lipoid S 100 were dissolved completely in ethanol in a water bath at 80 °C. The solvent was wiped off and the residue was quickly frozen at −20 °C for 2 h. Pluronic® F68 was dissolved in 100 mL water at 4 °C, then mixed with the residue, and ground to form a rough water dispersion. The dispersion was homogenized 9 times using a high-pressure homogenizer (PandaPlus 1001L, GEA Niro Soavi, Parma, Italia) under a pressure of 600 bar, and then cooled to room temperature.

3.5. Central composite design

The concentrations of Compritol® 888 ATO (X_1), Lipoid S 100 (X_2), and Pluronic F68 (X_3) were chosen as factors in the experimental design (Table 1). The EE (Y_1) of CBG and RBG, drug loading (Y_2), and mean particle size (Y_3) were used to optimize the SLN formulations.

The experimental runs are shown in Table 1. The multiple linear regression model used for the response surface was: $Y = b_0 + b_1X_1 + b_2X_2 + b_3X_3 \ldots$, where Y was the measured response associated with each factor level combination, b_0 was an intercept, b_1 to b_3 were the regression coefficients, and X_1 to X_3 were coded levels of independent variables. Analysis of variance (ANOVA) was used to verify the reliability of the model.

The desirability function for the response to be minimized was defined as follows: $di_{min} = (Y_{max} - Y_i)/(Y_{max} - Y_{min})$, where Y_{min} and Y_{max} represented the lowest and highest possible values, respectively, and Y_i was the experimental value. For a response to be maximized, the desirability function was defined as follows: $di_{max} = (Y_i - Y_{min})/(Y_{max} - Y_{min})$. The constraints were Y_1: $Y_{max} = 100\%$ (desirable EE) and $Y_{min} = 80\%$ (lowest acceptable EE); Y_2: $Y_{max} = 5\%$ (largest acceptable drug loading) and $Y_{min} = 0.5\%$ (desirable drug loading; from a practical viewpoint, much lower drug loading is not necessary as this would have little benefit on the drug effect of TV-SLN) (Hao et al. 2012); and Y_3: $Y_{max} = 300$ (largest acceptable particle size, above which the dispersion is not considered to consist of SLNs) and $Y_{min} = 30$ (desirable particle size). Among these constraints, Y_1 and Y_2 were maximized, whereas Y_3 was minimized. Overall desirability (OD) was calculated by combining the individual desirability values using the geometric mean, as reported previously (Zhang et al. 2009). The optimal surfaces for individual response variables were located by superimposing the contour plots for all the response variables.

3.6. Determination of encapsulation efficiency and drug loading

The centrifugal ultrafiltration method was used to investigate the EE (Xie et al. 2011). The TV-loaded SLN suspension was weighed precisely and transferred into a centrifugal ultrafiltration tube with a molecular-weight cutoff (MWCO) of 10 kDa (Shanghai Youqi Industrial Co. Ltd, Shanghai, China) and centrifuged (SIGMA 2-16K, Sartorius, Germany) at 11913 g for 20 min. The ultrafiltrate fluid containing CBG and RBG was determined directly using HPLC. The EE was calculated with the following formula: $EE\ (\%) = (W_t - W_f)/W_t \times 100$, in which W_t was the amount of CBG and RBG loaded in the SLN suspension, and W_f was the amount of drug in the ultrafiltrate fluid (Lu et al. 2006). Drug loading of the SLN suspension was calculated as follows: drug loading $(\%) = (W_t - W_f)/W_n \times 100$, with W_n being the total weight of the SLNs. The determinations were performed in triplicate in a total of 3 samples.

3.7. Characterization of TV-SLNs

The mean particle size of the prepared SLNs was measured using the dynamic light scattering (DLS) technique and a computerized Zetasizer Nano ZS90 (Malvern, UK). Measurements were performed in triplicate. The appearance of the SLNs was examined using a transmission electron microscope (Philips Tecnai 12; Philips, Amsterdam, The Netherlands). Samples were prepared for negative staining. Copper nets carrying formvar supporting film (Zhong Jing Ke Yi Technology Inc., Beijing, China) were placed onto a stencil plate. The SLN suspension was dropped gently onto the film, and the film was allowed to dry for 5 min. A drop of 2% uranyl acetate was then added to the film and allowed to dry for 5 min, after which the film was observed under a transmission electron microscope.

3.8. Cell culture

The HeLa and SKOV-3 cells were maintained at 37 °C and 5% CO_2 in a CO_2 incubator (Forma 3111; Thermo Fisher Scientific, Walther, MA, USA). The culture medium was extracted using a MicroPette Plus pipette and 1 mL of zymine solution that was added. After 3 min of digestion, the zymine solution

was wiped off and 5 mL of culture medium was used to wash the cells. The cell suspension was distributed into a new culture dish and 10 mL of fresh culture medium was added for subcultivation. The culture was maintained at 37 °C and 5% CO_2. All procedures were performed on a super-clean bench and sterile conditions were maintained.

3.9. Cell morphology

Cells were plated onto 6-well plates at a density of 1×10^6 per well and allowed to attach for 48 h. The medium was then replaced with an equal volume (2 mL) of fresh medium containing the mass concentrations of the extract as 5.88, 58.82, or 588.24 ng/mL from TV-SLN suspension, or 588.24 ng/mL of TV extract for comparison. After incubation for 24 h, the cells were observed under an inverted microscope (Olympus Corporation, Takatiho, Japan).

3.10. MTT assay

Cells were seeded into 96-well plates (1×10^4 per well) in 100 μL of culture medium for 4 h, and then incubated with various concentrations of TV-SLN or TV extract suspensions for 24, 48, and 72 h. After incubation, 50 μL of MTT solution was added to the plates and incubated for 4 h. The medium and MTT were then removed, and 150 μL of dimethylsulfoxide (DMSO) was added at room temperature for 10 min with shaking. Cell optical density (OD) was determined using a microplate reader (Thermo Labsystems Oy, Helsinki, Finland) at 490 nm (Luo et al. 2011, Sun et al. 2012). Cell inhibition was calculated as the percentage of MTT survival.

3.11. Cell cycle detection

The HeLa and SKOV-3 cells were plated onto 6-well plates at a density of 1×10^6 per well and allowed to attach for 72 h. The medium was replaced with an equal volume (2 mL) of fresh medium containing the mass concentrations of the extract as 5.88, 58.82, or 588.24 ng/mL from TV-SLN suspension, or 588.24 ng/mL of TV extract, and incubated for 24 h. The attached cells were harvested by trypsinization and washed twice with ice-cold PBS, then resuspended in ice-cold PBS, and fixed with 75% ethanol for 24 h. The ethanol was removed by centrifugation, and the cells were then washed once in PBS and stained with 1 mL of propidium iodide (PI)/Triton X-100 solution (containing 0.1% [w/w] Triton X-100, 200 μg/mL RNase A, and 50 μg/mL PI in PBS) in the dark at room temperature for 30 min. The stained cells were analyzed using a BD FACSCalibur Flow Cytometer in combination with BD Lysis II Software (Becton, Dickinson and Co., Franklin Lakes, NJ, USA).

3.12. Statistical analysis

Statistical analysis was performed by one-way ANOVA or multiple linear regression analysis using Statistical Product and Service Solutions software (SPSS, version 15.0, SPSS Inc., Chicago, IL, USA). The results were expressed as the mean ± SD and were considered statistically significant at a confidence interval of 95% ($p < 0.05$).

Acknowledgments: This work was financially supported by a grant (2010JW12) from Shanghai Education Committee, program (10XD14303900) from the Science and Technology Commission of Shanghai Municipality and by project (NCET08-0898) from the State Education Ministry of the PR China.

References

Baviskar DT, Amritkar AS, Chaudhari HS, Jain DK (2012) Modulation of drug release from nanocarriers loaded with a poorly water soluble drug (flurbiprofen) comprising natural waxes. Pharmazie 67: 701–705.

Brubacher JR, Ravikumar PR, Bania T, Heller MB, Hoffman RS (1996) Treatment of toad venom poisoning with digoxin-specific Fab fragments. Chest 110: 1282–1288.

Brubacher JR, Lachmanen D, Ravikumar PR, Hoffman RS (1999) Efficacy of digoxin specific Fab fragments (Digibind) in the treatment of toad venom poisoning. Toxicon 37: 931–942.

Cao-Hong, Shibayama-Imazu T, Masuda Y, Shinki T, Nakajo S, Nakaya K (2007) Involvement of Tiam1 in apoptosis induced by bufalin in HeLa cells. Anticancer Res 27: 245–249.

Castro GA, Coelho AL, Oliveira CA, Mahecha GA, Oréfice RL, Ferreira LA (2009) Formation of ion pairing as an alternative to improve encapsulation and stability and to reduce skin irritation of retinoic acid loaded in solid lipid nanoparticles. Int J Pharm 381: 77–83.

Chan WY, Ng TB, Yeung HW (1995) Examination for toxicity of a Chinese drug, the toad glandular secretory product chan su, in pregnant mice and embryos. Biol Neonate 67: 376–380.

Chen H, Chang X, Weng T, Zhao X, Gao Z, Yang Y, Xu H, Yang X (2004) A study of microemulsion systems for transdermal delivery of triptolide. J Control Release 98: 427–436.

Dhawan S, Kapil R, Singh B (2011) Formulation development and systematic optimization of solid lipid nanoparticles of quercetin for improved brain delivery. J Pharm Pharmacol 63: 342–351.

Goretti M, Branda E, Turchetti B, Cramarossa MR, Onofri A, Forti L, Buzzini P (2012) Response surface methodology as optimization strategy for asymmetric bioreduction of (4S)-(+)-carvone by *Cryptococcus gastricus*. Bioresour Technol 121: 290–297.

Guo X, Cui F, Xing Y, Mei Q, Zhang Z (2011) Investigation of a new injectable thermosensitive hydrogel loading solid lipid nanoparticles. Pharmazie 66: 948–952.

Haas JA, Witten MR, Clancey O, Episcopia K, Accordino D, Chalas E (2012) CyberKnife boost for patients with cervical cancer unable to undergo brachytherapy. Front Oncol 2: 25.

Hao J, Wang F, Wang X, Zhang D, Bi Y, Gao Y, Zhao X, Zhang Q (2012) Development and optimization of baicalin-loaded solid lipid nanoparticles prepared by coacervation method using central composite design. Eur J Pharm Sci 47: 497–505.

Jiang YM, Meng ZZ, Yue GX, Chen JX (2012) Norcantharidin induces HL-60 cells apoptosis *in vitro*. Evid Based Complement Alternat Med 2012: 154271.

Kakkar V, Singh S, Singla D, Kaur IP (2011) Exploring solid lipid nanoparticles to enhance the oral bioavailability of curcumin. Mol Nutr Food Res 55: 495–503.

Kaur IP, Bhandari R, Bhandari S, Kakkar V (2008) Potential of solid lipid nanoparticles in brain targeting. J Control Release 127: 97–109.

Lu B, Xiong SB, Yang H, Yin XD, Chao RB (2006) Solid lipid nanoparticles of mitoxantrone for local injection against breast cancer and its lymph node metastases. Eur J Pharm Sci 28: 86–95.

Luo WJ, Zhou Y, Liu MG, Wang CF (2011) Effect of basic fibroblast growth factor on cat corneal endothelial cell proliferation. Int J Ophthalmol 4: 384–387.

Ma XC, Zhang BJ, Xin XL, Huang SS, Deng S, Zhang HL, Shu XH, Diao YP, Cui J (2009) Simultaneous quantification of seven major bufadienolides in three traditional Chinese medicinal preparations of Chansu by HPLC-DAD. Nat Prod Commun 4: 179–184.

Ma H, Zhou J, Jiang J, Duan J, Xu H, Tang Y, Lv G, Zhang J, Zhan Z, Ding A (2012) The novel antidote Bezoar Bovis prevents the cardiotoxicity of toad (*Bufo bufo gargarizans* Canto) venom in mice. Exp Toxicol Pathol 64: 417–423.

Masuda Y, Kawazoe N, Nakajo S, Yoshida T, Kuroiwa Y, Nakaya K (1995) Bufalin induces apoptosis and influences the expression of apoptosis-related genes in human leukemia cells. Leuk Res 19: 549–556.

Minelli R, Serpe L, Pettazzoni P, Minero V, Barrera G, Gigliotti C, Mesturini R, Rosa AC, Gasco P, Vivenza N, Muntoni E, Fantozzi R, Dianzani U, Zara GP, Dianzani C (2012) Cholesteryl butyrate solid lipid nanoparticles inhibit the adhesion and migration of colon cancer cells. Br J Pharmacol 166: 587–601.

National Commission of Chinese Pharmacopoeia (2010) Pharmacopoeia of the People's Republic of China. Chemical Industry Press, second part, Beijing, p. 316.

Peng YM, Wang N, Wang YF, Han L, Zhang Y, Jiang JH, Zhou YB, Wang QD (2012) Correlation between reversing effect of cepharanthine hydrochloride on multidrug resistance and P-glycoprotein expression and function of K562/ADR cells. Yao Xue Xue Bao 47: 594–599.

Plummer PN, Freeman R, Taft R, Vider J, Sax M, Umer BA, Gao D, Johns CA, Mattick JS, Wilton SD, Ferro V, McMillan NA, Swarbrick A, Mittal V, Mellick AS (2012) MicroRNAs regular tumor angiogenesis modulated by endothelial progenitor cells. Cancer Res. doi: 10.1158/0008-5472.CAN-12-0271.[Epub ahead of print].

Qi J, Lu Y, Wu W (2012) Absorption, disposition and pharmacokinetics of solid lipid nanoparticles. Curr Drug Metab 13: 418–428.

Qureshi AA, Saavedra A (2011) Palmar fasciitis and polyarthritis syndrome in patients with ovarian cancer-a case report and review of the literature. Hand (NY) 6: 220–223.

Shegokar R, Singh KK (2011) Stavudine entrapped lipid nanoparticles for targeting lymphatic HIV reservoirs. Pharmazie 66: 264–271.

Shimizu Y, Inoue E, Ito C (2004) Effect of the water-soluble and non-dialyzable fraction isolated from senso (chan su) on lymphocyte proliferation and natural killer activity in C3H mice. Biol Pharm Bull 27: 256–260.

Silva AC, González-Mira E, García ML, Egea MA, Fonseca J, Silva R, Santos D, Souto EB, Ferreira D (2011) Preparation, characterization and biocompatibility studies on risperidone-loaded solid lipid nanoparticles (SLN): high pressure homogenization versus ultrasound. Colloids Surf B Biointerfaces 86: 158–165.

Sintov AC, Shapiro L (2004) New microemulsion vehicle facilitates percutaneous penetration *in vitro* and cutaneous drug bioavailability *in vivo*. J Control Release 95: 173–183.

Skarda J, Kolar Z, Janikova M, Radova L, Kolek V, Fridman E, Kopolovic J (2012) Analysis of the prognostic impact of nestin expression in non-small cell lung cancer. Biomed Pap Med Fac Univ Palacky Olomouc Czech Repub 156: 135–142.

Sun HW, Wu C, Tan HY, Wang QS (2012) Combination DLL4 with Jagged1-siRNA can enhance inhibition of the proliferation and invasiveness activity of human gastric carcinoma by Notch1/VEGF pathway. Hepatogastroenterology 59: 924–929.

Weyenberg W, Filev P, Van den Plas D, Vandervoort J, De Smet K, Sollie P, Ludwig A (2007) Cytotoxicity of submicron emulsions and solid lipid nanoparticles for dermal application. Int J Pharm 337: 291–298.

Xie S, Zhu L, Dong Z, Wang X, Wang Y, Li X, Zhou W (2011) Preparation, characterization and pharmacokinetics of enrofloxacin-loaded solid lipid nanoparticles: influences of fatty acids. Colloids Surf B Biointerfaces 83: 382–387.

Yamada K, Hino K, Tomoyasu S, Honma Y, Tsuruoka N (1998) Enhancement by bufalin of retinoic acid-induced differentiation of acute promyelocytic leukemia cells in primary culture. Leuk Res 22: 589–595.

Zhang J, Fan Y, Smith E (2009) Experimental design for the optimization of lipid nanoparticles. J Pharm Sci 98: 1813–1819.

Zhang X, Lü S, Han J, Sun S, Wang L, Li Y (2011) Preparation, characterization and *in vivo* distribution of solid lipid nanoparticles loaded with syringopicroside. Pharmazie 66: 404–407.

Zhuang YG, Xu B, Huang F, Wu JJ, Chen S (2012) Solid lipid nanoparticles of anticancer drugs against MCF-7 cell line and a murine breast cancer model. Pharmazie 67: 925–929.